Proc. Natl. Sci. Counc. ROC(A)
Vol. 21, No. 5, 1997. pp. 454-465

Time Simulation of Nonlinear Wave Loads on a Ship in Oblique Waves

MING-CHUNG FANG AND CHENG-MING LIAO

Department of Naval Architecture and Marine Engineering
National Cheng Kung University
Tainan, Taiwan, R.O.C.

(Received November 8, 1996; Accepted April 10, 1997)

ABSTRACT

In the paper, a prediction method for the nonlinear wave loads of a ship advancing in oblique waves with infinite water depth is proposed. Because of the good development in the hydrodynamics, the corresponding hydrodynamic coefficients and forces on ships can be well estimated. With this good basis, the authors consider the ship as a free-free beam and use the simple beam theory to estimate the corresponding sea loads along the ship hull, i.e., the wave bending moment, shear force and torsion moment at any ship section. Based on the well developed linear theory, an analytical model of the nonlinear wave loads for a ship in large oblique waves is further constructed. Time domain analyses, including the instant grid generation technique (IGGT), for the corresponding sea loads are performed. Furthermore, to avoid the numerical drift phenomena in the sway and yaw mode motions, the Artificial Restoring Force Technique(ARFT) and Digital Filter Technique(DFT) are applied to solve five coupled equations of motion. A series of analyses is performed in this paper, and some valuable suggestions are also submitted The calculation procedures developed here may be considered as an efficient analytical tool for researchers to predict the ship motions and wave induced loads.

Key Words: nonlinear wave loads, time domain, digital filter

I. Introduction

Dynamic wave load prediction is very important for the structural analysis of a ship moving in waves. Before the tool for dynamic analysis was well developed, the naval architect usually used the ship's effective power performance in calm water and the ship's maximum bending moment in the static "One-over-twenty" wave as the main design criteria. However, after the ship hydrodynamics are carefully studied, the dynamic wave loads can then be widely applied for the ship design.

Since Korvin-Kroukovsky (1955) first used the strip theory to calculate the heave and pitch motion of a ship in head waves, the strip theory has been widely applied to analyze ship motion and wave loads. Jacobs (1958) was first to calculate the vertical shear force and the vertical bending moment on a ship using the theory developed by Korvin-Kroukovsky (1955). Although the original strip theory (Korvin-Kroukovsky, 1955) was based on "physical intuition," it was proved to be one of the most significant contributions in the field of seakeeping. Later, Gerritsma and Beukelman (1967) proposed a modified strip theory, in which computations of the sectional added mass and damping coefficients were improved by using the close-fit methods. Tasai and Takaki (1969) derived another new strip theory for predicting heave and pitch motions, which have identical forward-speed terms satisfying the Timman and Newman symmetry relationships. Salvesen *et al.* (1970) used a new potential theory to solve the ship motions and sea loads in regular waves, and its validity was proven through comparison with experimental data (Wahab, 1967). Using the same diffraction theory and different hydrodynamic force formulas, i.e., the Haskind-Newman relationship approach, Wahab and Vink (1975) derived another method to calculate sea loads and verified it using previous experimental data (Wahab, 1967). Kim *et al.* (1980) developed another strip method to estimate ship motions, hydrodynamic pressure distribution and sea loads by using a different diffraction theory, in which the diffraction force is calculated directly by satisfying the diffraction boundary condition on a hull surface. Because the linear mathematical model of Kim *et al.* (1980) has been proven to be very useful in many aspects of seakeeping, the authors (Fang and Liao, 1996) used this method to calculate the corresponding wave loads in the frequency domain, in which some corrections were made in the original formulas for

horizontal shear force, horizontal bending moment and torsion moment. Comparisons with experimental data and other theories were also made, and the agreement is generally satisfactory.

However, the theories with the small amplitude assumption stated above are inadequate if large waves are considered. Recently, the nonlinear effects of large waves on ship motions and wave loads have been extensively studied by some authors, e.g., Ohtsubo *et al.* (1985) and Fujino and Yoon (1986). It would be more practical to use the large wave amplitude concept to predict the wave loads. Bϕrresen and Tellsgard (1980) used time domain simulation to analyze nonlinear ship motions and wave loads in longitudinal waves, but oblique wave cases were not considered. Fang *et al.* (1993) developed a well technique to simulate motion and water shipping for a ship advancing in longitudinal waves, and it was also applied to SWATH ship motion analysis in longitudinal waves (Fang and Her, 1995). Both results were well confirmed by experimental data. Therefore, this technique was extended to analyze ship motions in oblique waves by Chen (1994). In the present study, by combining the ship motion prediction model in oblique waves (Chen,1994) with formulas for wave loads (Fang and Liao,1996), the authors develop a time simulation technique for predicting nonlinear wave loads on a ship advancing in oblique waves. To reduce the calculation time, the instant grid generation technique (Chen, 1994) is applied to calculate the corresponding hydrodynamic coefficients in the time domain. An artificial restoring force technique and a digital filter technique are also included to avoid the numerical drifting phenomena. The general corresponding mathematical formulas are described as in the following sections.

II. Equations of Motions in Time Domain

Before dealing with the equations of motions, some assumptions about the flow must be made. The flow is assumed to be incompressible, inviscid and irrotational. The water depth is assumed to be infinite, and the ship is advancing in regular waves with constant speed.

Because the nonlinear effects of the large amplitude are considered here, all the related hydrodynamic coefficients become time dependent. Then, by neglecting the effect of the surge mode, the five modes of motions are all coupled, and the equations of motions must be written as follows.

(1) Heave mode (ζ):

$$(M+M''_{\zeta\zeta}(t))\ddot{\zeta}+N_{\zeta\zeta}(t)\dot{\zeta}+B_{\zeta\zeta}(t)\zeta+M''_{\psi\zeta}(t)\ddot{\psi}+N_{\psi\zeta}(t)\dot{\psi}$$
$$+B_{\psi\zeta}(t)\psi+M''_{\eta\zeta}(t)\ddot{\eta}+N_{\eta\zeta}(t)\dot{\eta}+B_{\eta\zeta}(t)\eta+M''_{\chi\zeta}(t)\ddot{\chi}$$
$$+N_{\chi\zeta}(t)\dot{\chi}+B_{\chi\zeta}(t)\chi+M''_{\phi\zeta}(t)\ddot{\phi}+N_{\phi\zeta}(t)\dot{\phi}+B_{\phi\zeta}(t)\phi$$
$$=\mathrm{Re}\{F_\zeta(t)\}+R_\zeta(t); \quad (1)$$

(2) Pitch mode (ψ):

$$M''_{\zeta\psi}(t)\ddot{\zeta}+N_{\zeta\psi}(t)\dot{\zeta}+B_{\zeta\psi}(t)\zeta+(I_{\psi\psi}+M''_{\psi\psi}(t))\ddot{\psi}$$
$$+N_{\psi\psi}(t)\dot{\psi}+B_{\psi\psi}(t)\psi+M''_{\eta\psi}(t)\ddot{\eta}+N_{\eta\psi}(t)\dot{\eta}+B_{\eta\psi}(t)\eta$$
$$+M''_{\chi\psi}(t)\ddot{\chi}+N_{\chi\psi}(t)\dot{\chi}+B_{\chi\psi}(t)\chi+M''_{\phi\psi}(t)\ddot{\phi}+N_{\phi\psi}(t)\dot{\phi}$$
$$+B_{\phi\psi}(t)\phi=\mathrm{Re}\{F_\psi(t)\}+R_\psi(t); \quad (2)$$

(3) Sway mode (η):

$$M''_{\zeta\eta}(t)\ddot{\zeta}+N_{\zeta\eta}(t)\dot{\zeta}+B_{\zeta\eta}(t)\zeta+M''_{\psi\eta}(t)\ddot{\psi}+N_{\psi\eta}(t)\dot{\psi}$$
$$+B_{\psi\eta}(t)\psi+(M+M''_{\eta\eta}(t))\ddot{\eta}+N_{\eta\eta}(t)\dot{\eta}+B_{\eta\eta}(t)\eta$$
$$+M''_{\chi\eta}(t)\ddot{\chi}+N_{\chi\eta}(t)\dot{\chi}+B_{\chi\eta}(t)\chi+M''_{\phi\eta}(t)\ddot{\phi}+N_{\phi\eta}(t)\dot{\phi}$$
$$+B_{\phi\eta}(t)\phi=\mathrm{Re}\{F_\eta(t)\}; \quad (3)$$

(4) Yaw mode (χ):

$$(M''_{\zeta\chi}(t))\ddot{\zeta}+N_{\zeta\chi}(t)\dot{\zeta}+B_{\zeta\chi}(t)\zeta+M''_{\psi\chi}(t)\ddot{\psi}+N_{\psi\chi}(t)\dot{\psi}$$
$$+B_{\psi\chi}(t)\psi+M''_{\eta\chi}(t)\ddot{\eta}+N_{\eta\chi}(t)\dot{\eta}+B_{\eta\chi}(t)\eta$$
$$+(I_{\chi\chi}+M''_{\chi\chi}(t))\ddot{\chi}+N_{\chi\chi}(t)\dot{\chi}+B_{\chi\chi}(t)\chi$$
$$+M''_{\phi\chi}(t)\ddot{\phi}+N_{\phi\chi}(t)\dot{\phi}+B_{\phi\chi}(t)\phi=\mathrm{Re}\{F_\chi(t)\}; \quad (4)$$

(5) Roll mode (ϕ):

$$M''_{\zeta\phi}(t)\ddot{\zeta}+N_{\zeta\phi}(t)\dot{\zeta}+B_{\zeta\phi}(t)\zeta+M''_{\psi\phi}(t)\ddot{\psi}+N_{\psi\phi}(t)\dot{\psi}$$
$$+B_{\psi\phi}(t)\psi+M''_{\eta\phi}(t)\ddot{\eta}+N_{\eta\phi}(t)\dot{\eta}+B_{\eta\phi}(t)\eta+M''_{\chi\phi}(t)\ddot{\chi}$$
$$+N_{\chi\phi}(t)\dot{\chi}+B_{\chi\phi}(t)\chi+(M+M''_{\phi\phi}(t))\ddot{\phi}+N_{\phi\phi}(t)\dot{\phi}$$
$$+B_{\phi\phi}(t)\phi=\mathrm{Re}\{F_\phi(t)\}, \quad (5)$$

where M'', N and B represent the added mass, damping coefficient and restoring force, respectively. The first subscript represents the mode of motions and the second one represents the direction of force. F is the exciting force. M is the ship mass.

The corresponding hydrodynamic coefficients are varied with time, and the treatment of these coefficients can be found by referring to Fang *et al.* (1993) or

referred to Chen (1994). The former used the least-square-fit method and the latter used the instant grid generation technique (IGGT). Because the technique used by Fang *et al.* (1993) is labor-consuming for oblique waves, we adapt the IGGT (Chen, 1994) in the present study. The corresponding hydrodynamic coefficients will be automatically calculated based on the different hull shape at each time step.

III. Wave Loads in the Time Domain

Generally, the wave loads for a ship advancing in waves are due to the following five components: (1) the ship weight or ship inertia force, (2) the Froude-Krylov force due to incident waves, (3) the diffraction force, (4) the hydrodynamic inertia force, i.e., added mass, and damping force, and (5) the restoring force.

Regarding the ship as a free-free beam, we can use the simple beam theory in material mechanics to calculate the corresponding sectional sea loads along the ship's hull length. The ship is in motion, and the dynamic equilibrium method, i.e., the D'Alembert principle, can be used to calculate the corresponding sea loads at any ship section. The corresponding sea loads, including the vertical shear force (F_v), vertical bending moment (M_v), horizontal shear force (F_L), horizontal bending moment (M_L) and torsion moment (M_T), are shown in Fig. 1.

The resultant sectional force and moment due to the vertical motion, horizontal motion and roll motion in large waves are shown in the following formulas.

(1) Sectional vertical force:

$$\begin{aligned} &K_\zeta(x,t) \\ &= K_{He}(x,t) - \{(m_o(x,t) + M''_{HH}(x,t))\ddot{\zeta} + N_{HH}(x,t)\dot{\zeta}\} \\ &\quad + R_\zeta(x,t) \\ &\quad - \{(-xm_o(x,t) - xM''_{HH}(x,t))\ddot{\psi} - xN_{HH}(x,t)\dot{\psi}\} \\ &\quad - \{M''_{SH}(x,t)\ddot{\eta} + N_{SH}(x,t)\dot{\eta}\} \\ &\quad - \{xM''_{SH}(x,t)\ddot{\chi} + xN_{SH}(x,t)\dot{\chi}\} \\ &\quad - \{(m_o(x,t)Z_{cx}(x,t) + M''_{RH}(x,t))\ddot{\phi} + N_{RH}(x,t)\dot{\phi}\}; \end{aligned} \tag{6}$$

(2) Sectional horizontal force:

$$\begin{aligned} &K_\eta(x,t) \\ &= K_{Se}(x,t) - \{M''_{HS}(x,t)\ddot{\zeta} + N_{HS}(x,t)\dot{\zeta}\} \\ &\quad - \{-xM''_{HS}(x,t)\psi - xN_{HS}(x,t)\dot{\psi}\} \\ &\quad - \{(m_o(x,t) + M''_{SS}(x,t))\ddot{\eta} + N_{SS}(x,t)\dot{\eta}\} \\ &\quad - \{(xm_o(x,t) + xM''_{SS}(x,t))\ddot{\chi} + xN_{SS}(x,t)\dot{\chi}\} \\ &\quad - \{(m_o(x,t)Z_{cy}(x,t) + M''_{RS}(x,t))\ddot{\phi} + N_{RS}(x,t)\dot{\phi}\}; \end{aligned} \tag{7}$$

(3) Sectional roll moment:

$$\begin{aligned} &K_\phi(x,t) \\ &= K_{Re}(x,t) - \{(m_o(x,t)Z_{cx}(x,t) + M''_{HR}(x,t))\ddot{\zeta} \\ &\quad + N_{HR}(x,t)\dot{\zeta}\} \\ &\quad - \{(-xm_o(x,t)Z_{cx}(x,t) - xM''_{HR}(x,t))\ddot{\psi} \\ &\quad - xN_{HR}(x,t)\dot{\psi}\} \\ &\quad - \{(m_o(x,t)Z_{cy}(x,t) + M''_{SR}(x,t))\ddot{\eta} + N_{SR}(x,t)\dot{\eta}\} \\ &\quad - \{(xm_o(x,t)Z_{cy}(x,t) + xM''_{SR}(x,t))\ddot{\chi} + xN_{SR}(x,t)\dot{\chi}\} \\ &\quad - \{(I_o(x,t) + M''_{RR}(x,t))\ddot{\phi} + N_{RR}(x,t)\dot{\phi}\} - R_\phi(x,t)\phi, \end{aligned} \tag{8}$$

where

$m_o(x,t)$= instantaneous sectional mass;

$Z_{cy}(x,t)$=the vertical distance between the instantaneous centroid and the center of gravity; "+" means that the centroid is below the center of gravity;

$Z_{cx}(x,t)$=the horizontal distance between the instantaneous centroid and the center of

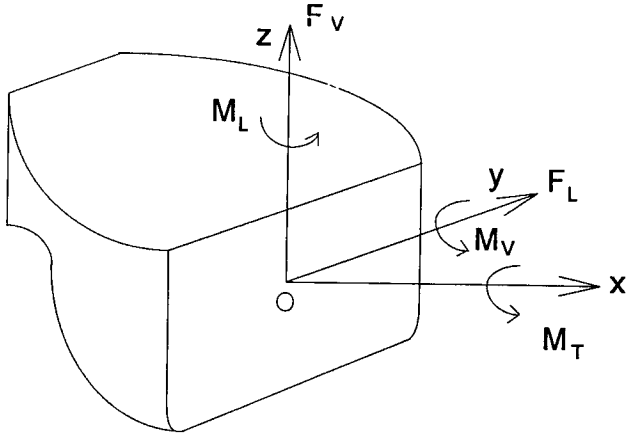

Fig. 1. A diagram for the definitions of sea loads.

gravity; "+" means that the centroid is to the right of the center of gravity;

$xm_o(x,t)\ddot{\psi}$= instantaneous sectional vertical inertial force due to pitch;

$xm_o(x,t)\ddot{\chi}$= instantaneous sectional horizontal inertial force due to yaw;

$m_o(x,t)Z_{cx}(x,t)\ddot{\phi}$= instantaneous sectional horizontal inertial force due to roll;

$m_o(x,t)Z_{cy}(x,t)\ddot{\phi}$= instantaneous sectional vertical inertial force due to roll;

$m_o(x,t)Z_{cx}(x,t)(\ddot{\zeta}-x\ddot{\psi})$= instantaneous sectional horizontal inertial force due to roll;

$m_o(x,t)Z_{cy}(x,t)(\ddot{\eta}+x\ddot{\chi})$= instantaneous sectional vertical inertial force due to roll;

$I_o(x,t)\ddot{\phi}$=moment inertia force due to roll;

$R_\zeta(x,t)$= instantaneous restoring force per unit heave;

$R_\phi(x,t)$= instantaneous restoring moment per unit roll;

$K_{He}(x,t)$=instantaneous heave exciting force;

$K_{Se}(x,t)$= instantaneous sway exciting force;

$K_{Re}(x,t)$=instantaneous roll exciting moment.

In order to evaluate the sea loads on an arbitrary section at $x=x_0$, fore or aft from the longitudinal center of gravity, we assume another variable x in $x=\xi+x_0$, where $x_0>0$ for a fore section. Then, integrating the above three equations from x_0 to bow, we can obtain the wave loads at any section x_0 as follows.

(1) Vertical shear force:

$$
\begin{aligned}
&F_V(x,t)\\
&=\int_o^{L_2} K_\zeta(\xi+x_o,t)\,d\xi\\
&=\int_o^{L_2} K_{He}(\xi+x_o,t)\,d\xi-\{(\int_o^{L_2} m_o d\xi+\int_o^{L_2} M''_{HH}d\xi)(\ddot{\zeta}-x_o\ddot{\psi})\}\\
&-(\int_o^{L_2} N_{HH}d\xi)(\dot{\zeta}-x_o\dot{\psi})+\int_o^{L_2} R_\zeta d\xi\\
&-\{(-\int_o^{L_2}\xi m_o d\xi-\int_o^{L_2}\xi M''_{HH}d\xi)\ddot{\psi}+(-\int_o^{L_2}\xi N_{HH}d\xi)\dot{\psi}\}\\
&-\{(\int_o^{L_2} M''_{SH}d\xi)(\ddot{\eta}+x_o\ddot{\chi})+(\int_o^{L_2} N_{SH}d\xi)(\dot{\eta}+x_o\dot{\chi})\}\\
&-\{(-\int_o^{L_2}\xi M''_{SH}d\xi)\ddot{\chi}+(-\int_o^{L_2}\xi N_{SH}d\xi)\dot{\chi}\}\\
&-\{(\int_o^{L_2} m_o Z_{cx}d\xi+\int_o^{L_2} M''_{RH}d\xi)\ddot{\phi}+(\int_o^{L_2} N_{RH}d\xi)\dot{\phi}\};
\end{aligned}
\tag{9}
$$

(2) Vertical bending moment:

$$
\begin{aligned}
&M_V(x,t)\\
&=-\int_o^{L_2}\xi K_\zeta(\xi+x_o,t)\,d\xi\\
&=-\int_o^{L_2}\xi K_{He}(\xi+x_o,t)\,d\xi-\{(-\int_o^{L_2}\xi m_o d\xi-\int_o^{L_2}\xi M''_{HH}d\xi)\ddot{\zeta}\\
&+(-\int_o^{L_2}\xi N_{HH}d\xi)\dot{\zeta}\}-\int_o^{L_2}\xi R_\zeta d\xi\\
&-x_o\{(\int_o^{L_2}\xi m_o d\xi+\int_o^{L_2}\xi M''_{HH}d\xi)\ddot{\psi}+(\int_o^{L_2}\xi N_{HH}d\xi)\dot{\psi}\}\\
&-\{(\int_o^{L_2}\xi^2 m_o d\xi+\int_o^{L_2}\xi^2 M''_{HH}d\xi)\ddot{\psi}+(\int_o^{L_2}\xi^2 N_{HH}d\xi)\dot{\psi}\}\\
&-\{(-\int_o^{L_2}\xi M''_{SH}d\xi)\ddot{\eta}+(-\int_o^{L_2}\xi N_{SH}d\xi)\dot{\eta}\}\\
&-x_o\{(-\int_o^{L_2}\xi M''_{SH}d\xi)\ddot{\chi}+(-\int_o^{L_2}\xi N_{SH}d\xi)\dot{\chi}\}\\
&-\{(-\int_o^{L_2}\xi^2 M''_{SH}d\xi)\ddot{\chi}+(-\int_o^{L_2}\xi^2 N_{SH}d\xi)\dot{\chi}\}\\
&-\{(-\int_o^{L_2}\xi m_o Z_{cx}d\xi-\int_o^{L_2}\xi M''_{RH}d\xi)\ddot{\phi}\\
&+(-\int_o^{L_2}\xi N_{RH}d\xi)\dot{\phi}\};
\end{aligned}
\tag{10}
$$

(3) Horizontal shear force:

$$
\begin{aligned}
&F_L(x,t)\\
&=\int_o^{L_2} K_\eta(\xi+x_o,t)\,d\xi\\
&=\int_o^{L_2} K_{Se}(\xi+x_o,t)\,d\xi-\{(\int_o^{L_2} M''_{HS}d\xi)(\ddot{\zeta}-x_o\ddot{\psi})
\end{aligned}
$$

$$+\left(\int_o^{L_2} N_{HS}d\xi\right)(\dot{\zeta}-x_o\dot{\psi})\}$$

$$-\{(-\int_o^{L_2}\xi M''_{HS}d\xi)\ddot{\psi}+(-\int_o^{L_2}\xi N_{HS}d\xi)\dot{\psi}\}$$

$$-\{(\int_o^{L_2} m_o d\xi+\int_o^{L_2} M''_{SS}d\xi)(\ddot{\eta}+x_o\ddot{\chi})$$

$$+\left(\int_o^{L_2} N_{SS}d\xi\right)(\dot{\eta}+x_o\dot{\chi})\}$$

$$-\{(\int_o^{L_2}\xi m_o d\xi+\int_o^{L_2}\xi M''_{SS}d\xi)\ddot{\chi}+(\int_o^{L_2}\xi N_{SS}d\xi)\dot{x}\}$$

$$-\{(\int_o^{L_2} m_o Z_{cy}d\xi+\int_o^{L_2} M''_{RS}d\xi)\ddot{\phi}+(\int_o^{L_2} N_{RS}d\xi)\dot{\phi}\}; \quad \textbf{(11)}$$

(4) Horizontal bending moment:

$$M_L(x,t)$$

$$=\int_o^{L_2}\xi K_\eta(\xi+x_o,t)\,d\xi$$

$$=\int_o^{L_2}\xi K_{Se}(\xi+x_o,t)\,d\xi$$

$$-\{(\int_o^{L_2}\xi M''_{HS}d\xi)\ddot{\zeta}+(\int_o^{L_2}\xi N_{HS}d\xi)\dot{\zeta}\}$$

$$-x_o\{(-\int_o^{L_2}\xi M''_{HS}d\xi)\ddot{\psi}+(-\int_o^{L_2}\xi N_{HS}d\xi)\dot{\psi}\}$$

$$-\{(-\int_o^{L_2}\xi^2 M''_{HS}d\xi)\ddot{\psi}+(-\int_o^{L_2}\xi^2 N_{HS}d\xi)\dot{\psi}\}$$

$$-\{(\int_o^{L_2}\xi m_o d\xi+\int_o^{L_2}\xi M''_{SS}d\xi)\ddot{\eta}+(\int_o^{L_2}\xi N_{SS}d\xi)\dot{\eta}\}$$

$$-x_o\{(\int_o^{L_2}\xi m_o d\xi+\int_o^{L_2}\xi M''_{SS}d\xi)\ddot{\chi}+(\int_o^{L_2}\xi N_{SS}d\xi)\dot{\chi}\}$$

$$-\{(\int_o^{L_2}\xi^2 m_o d\xi+\int_o^{L_2}\xi^2 M''_{SS}d\xi)\ddot{\chi}+(\int_o^{L_2}\xi^2 N_{SS}d\xi)\dot{\chi}\}$$

$$-\{(\int_o^{L_2}\xi m_o Z_{cy}d\xi+\int_o^{L_2}\xi M''_{RH}d\xi)\ddot{\phi}+(\int_o^{L_2}\xi N_{RS}d\xi)\dot{\phi}\}; \quad \textbf{(12)}$$

(5) Torsion moment:

$$M_T(x,t)$$

$$=\int_o^{L_2} K_\phi(\xi+x_o,t)\,d\xi$$

$$=\int_o^{L_2} K_{Re}(\xi+x_o,t)\,d\xi-\{(\int_o^{L_2} m_o Z_{cx}d\xi$$

$$+\int_o^{L_2} M''_{HR}d\xi)(\ddot{\zeta}-x_o\ddot{\psi})+(\int_o^{L_2} N_{HR}d\xi)(\dot{\zeta}-x_o\dot{\psi})\}$$

$$-\{(-\int_o^{L_2}\xi m_o Z_{cx}d\xi-\int_o^{L_2}\xi M''_{HR}d\xi)\ddot{\psi}$$

$$+(-\int_o^{L_2}\xi N_{HR}d\xi)\dot{\psi}\}$$

$$-\{(\int_o^{L_2} m_o Z_{cy}d\xi+\int_o^{L_2} M''_{SR}d\xi)(\ddot{\eta}+x_o\ddot{\chi})$$

$$+\left(\int_o^{L_2} N_{SR}d\xi\right)(\dot{\eta}+x_o\dot{\chi})\}$$

$$-\{(\int_o^{L_2}\xi m_o Z_{cy}d\xi+\int_o^{L_2}\xi M''_{SR}d\xi)\ddot{\chi}+(\int_o^{L_2}\xi N_{SR}d\xi)\dot{\chi}\}$$

$$-\{(\int_o^{L_2} I_o d\xi+\int_o^{L_2} M''_{RR}d\xi)\ddot{\phi}+(\int_o^{L_2} N_{RR}d\xi)\dot{\phi}\}-(\int_o^{L_2} R_\phi d\xi)\phi. \quad \textbf{(13)}$$

In the above integration, the underwater shape is different at any instant time; therefore, every coefficient in the equation is a function of the time or shape position. L_2 indicates the distance between the section of interest and the fore end of the hull.

IV. Methods for Avoiding Numerical Drift

Some numerical drifting phenomena will occur in the sway and yaw modes when we solve the five coupled equations. To show how to avoid this, two methods are used here:(1) the Artificial Restoring Force Tech-

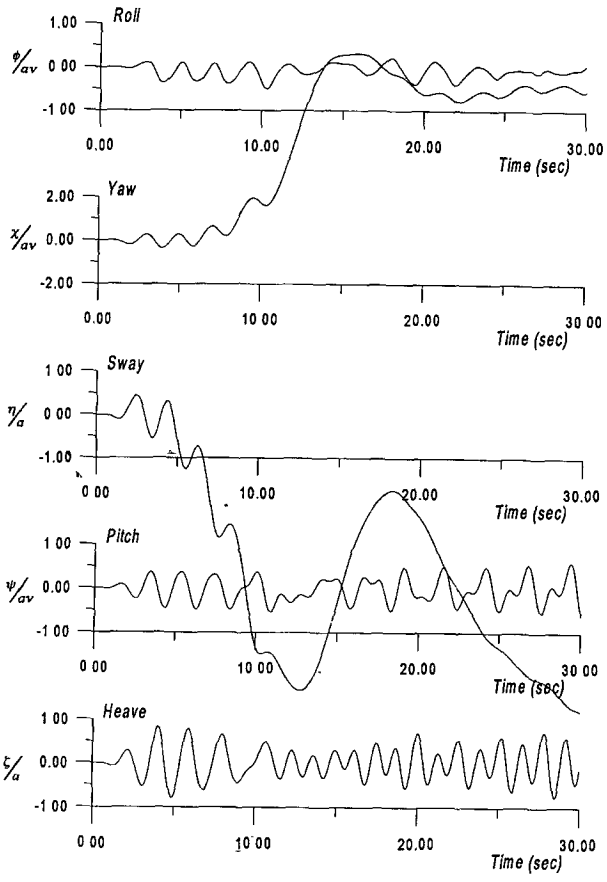

Fig. 2. Time histories of ship motions without using AFRT or DFT (μ=60°, λ/L=1.0, H/λ=1/30, Fr=0.15).

nique, ARFT; (2) the Digital Filter Technique, DFT.

1. Artificial Restoring Force Technique (ARFT)

The method is to add an artificial restoring force and moment in the sway and yaw equations. The artificial force is related to the encounter frequency and the ship mass. The formula is

$$k=(n\omega)^2 M, \tag{14}$$

where ω is the encounter frequency, M is the ship mass for the sway or the moment of inertia for yaw, and n is the coefficient to be determined.

2. Digital Filter Technique (DFT)

Because the general solution for the frequency causing the drift phenomena is zero and the required particular solution is equivalent to the encounter frequency, we only need to eliminate those frequencies which are lower than the required encounter frequency in the integration procedure. Therefore, the function of the filter used in the signal processing is applied in the present numerical calculation.

Generally, there are two kinds of digital filters: (1) the FIR (Finite Impulse Response) filter and (2) the IIR (Infinite Impulse Response) filter. In order to make the phase constant and avoid wave distortion, we adopt the FIR filter. In addition, the higher order filter must be used to obtain a sensitive truncation amplitude. Using the FIR filter, the signal processing can be expressed as

$$\{p\}_j = \sum_{i=0}^{N} h(i) \cdot \{P\}_{j-\frac{N}{2}+1+i}, \tag{15}$$

where N is the number of filters, $h(i)$ is the coefficient of the filter, and $\{p\}_j$ represents the output signal at step j. The coefficient of the filter can be calculated using

$$h(i) = \frac{k(i)}{k(0) + \sum_{i=1}^{N/2} 2k(i)} \quad \text{if } i=1\sim N/2$$

$$h(i) = h(\frac{N}{2} - j)_{j=1\sim\frac{N}{2}} \quad \text{if } i=N/2+1\sim N \tag{16}$$

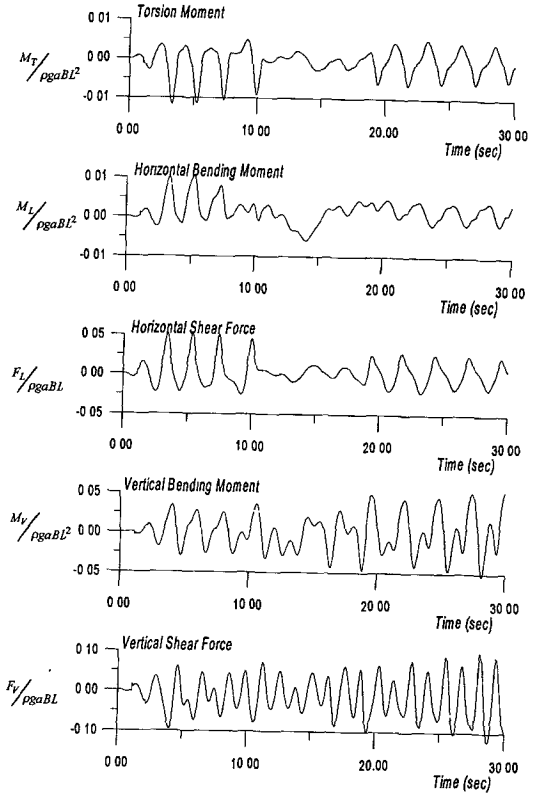

Fig. 3. Time histories of wave loads without using AFRT or DFT (μ=60°, λ/L=1.0, H/λ=1/30, Fr=0.15).

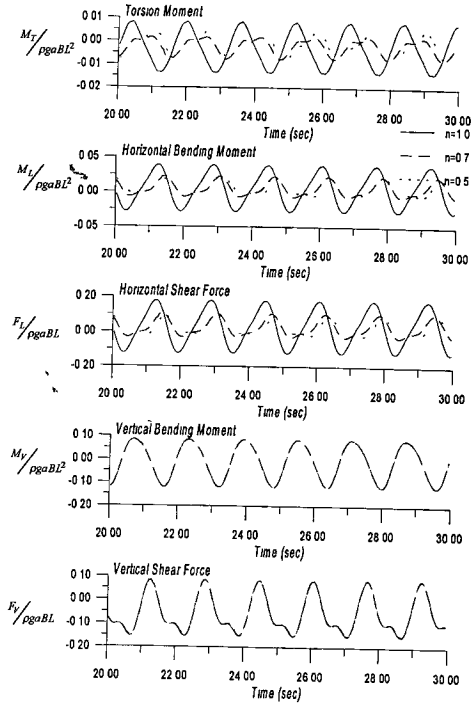

Fig. 4. Time histories of wave loads using AFRT with different artificial restoring coefficients (μ=90°, λ/L=1.0, H/λ=1/30, Fr=0.0).

$$\begin{cases} i=0 \Rightarrow k(i)=\dfrac{2f_c}{f_s} \\ i\neq 0 \Rightarrow k(i)=\dfrac{1}{i\pi}\sin(2i\pi\dfrac{f_c}{f_s})\cdot w_B(i), \end{cases} \tag{17}$$

where f_c is the truncation frequency, and f_s is the sampling frequency. $w_B(i)$ is Blackman window function and can be expressed as

$$w_B(i)=0.42+0.5\cos(\frac{2\pi i}{N+1})+0.08\cos(\frac{4\pi i}{N+1}). \tag{18}$$

Assume that the value at step j is known; then the value at the next step j+1 can be calculated using the following procedure:

(1) Take the displacement and velocity at step (j–N/2+1) as the initial value and proceed with time integration for N steps to obtain the displacement and velocity at each step j.

(2) Apply the low pass filter to the N+1 numbers of the calculated values for the N+1 displacements and velocities, and then subtract the value obtained from step (N/2) in procedure (1) from the output value obtained here.

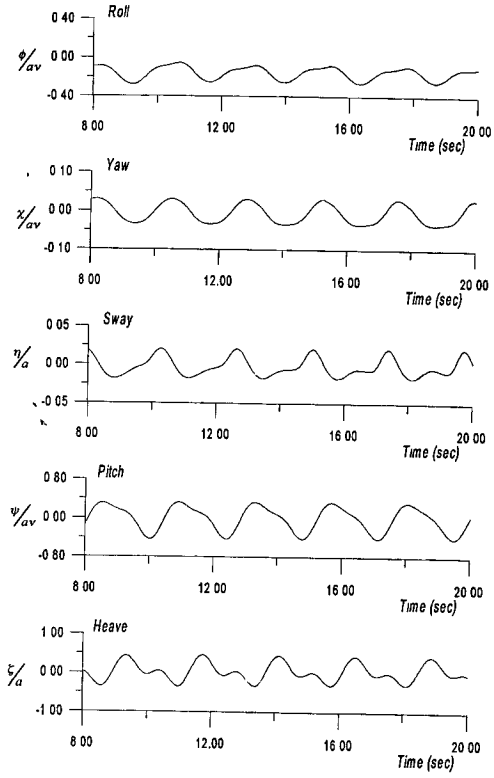

Fig. 5. Time histories of nondimensional ship motions (μ=30°, λ/L=1.0, H/λ=1/20, Fr=0.15).

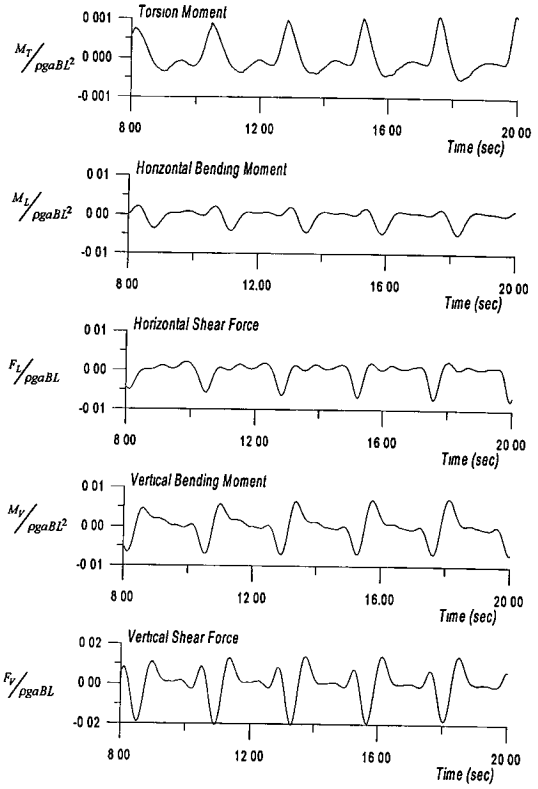

Fig. 6. Time histories of nondimensional wave loads (μ=30°, λ/L=1.0, H/λ=1/20, Fr=0.15).

(3) Substitute the value obtained in procedure (2) into the equations of motions and loads to get the solution at step $j+1$.
(4) Proceed to the next time step, and repeat the above procedure, (1) (2) (3), again.

V. Results and Discussion

The validity of the present theory in linear application has been confirmed previously in the frequency domain (Fang and Liao, 1996). To simplify this presentation, we will only show the nonlinear analysis with large wave amplitude by means of time simulation. The Series 60 ship with C_b=0.8 was selected as the numerical model for calculating the ship motions and wave loads at the midship section. In the following figures, all the results are nondimensionalized by the corresponding variables: a (wave amplitude), L (ship length), B (ship breadth), g (gravitational acceleration), ρ (water density), and ν (wave number).

Figures 2 and 3 show the results of the ship motions and wave loads in oblique waves without using ARFT or DFT. We can see that the numerical drifting phenomena occurred in sway and yaw mo-

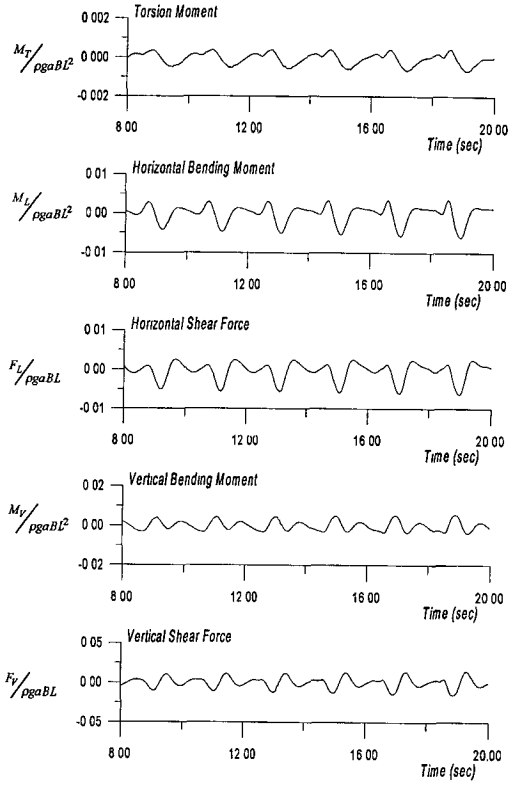

Fig. 8. Time histories of nondimensional wave loads (μ=60°, λ/L=1.0, H/λ=1/30, Fr=0.15).

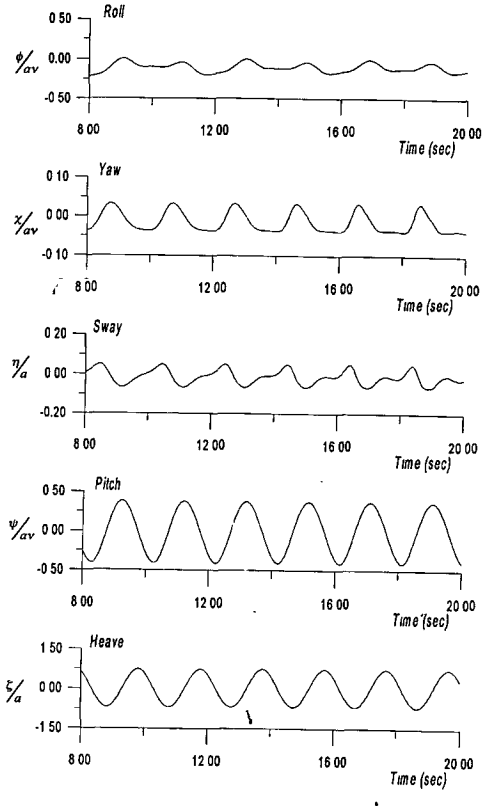

Fig. 7. Time histories of nondimensional ship motions (μ=60°, λ/L=1.0, H/λ=1/30, Fr=0.15).

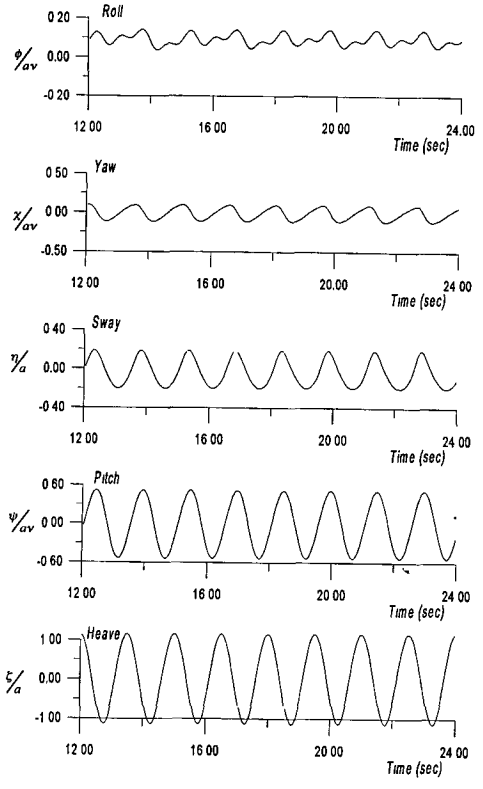

Fig. 9. Time histories of nondimensional ship motions (μ=120°, λ/L=1.0, H/λ=1/30, Fr=0 05).

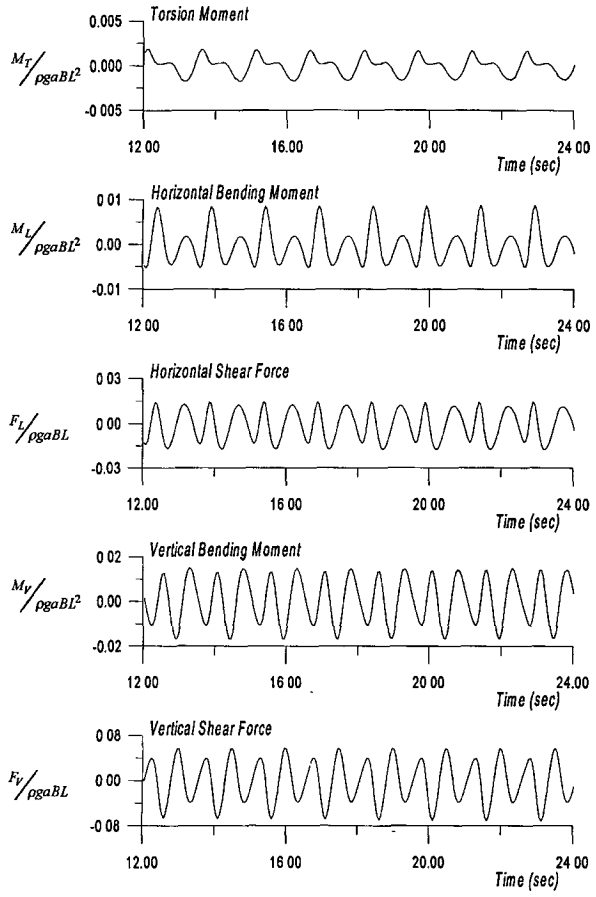

Fig. 10. Time histories of nondimensional wave loads (μ=120°, λ/L=1.0, H/λ=1/30, Fr=0.05).

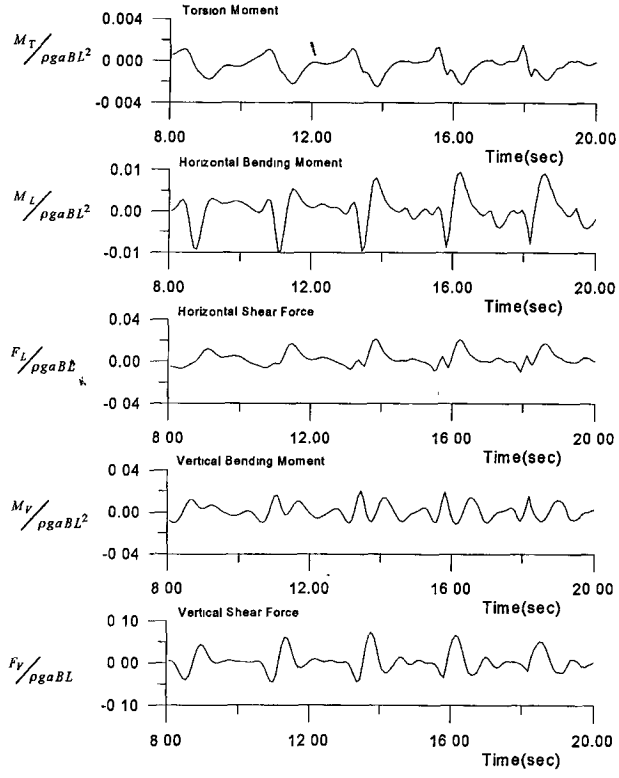

Fig. 11. Time histories of nondimensional wave loads (μ=30°, λ/L=1.0, H/λ=1/20, Δt=T/30, N=30, Fr=0.15).

tions, which led to unstable results in the wave loads simulation. Therefore, techniques such as ARFT or DFT must be applied to avoid the drifting phenomena. Figure 4 shows the application of ARFT to the beam wave case. The results are indeed quite stable. Although the results for the horizontal mode vary with different artificial restoring coefficients, there is almost no influence on the vertical modes. Because the artificial restoring force was an external force that caused discontinuity when we drew the diagrams for the shear force and bending moment along the ship's length, we then used DFT.

Figures 5 and 6 show the results of the time simulation for the ship motions and wave loads at μ=30° with Fr=0.15, λ/L=1.0 and H/λ=1/20 (μ is the wave direction, λ is the wave length, and H is the wave height). From both figures, we can see the results are fairly stable. Generally, the result for each time history is not symmetric with respect to the zero level, which is a general phenomena in large amplitude analysis. In particular, the roll motion mode oscillates

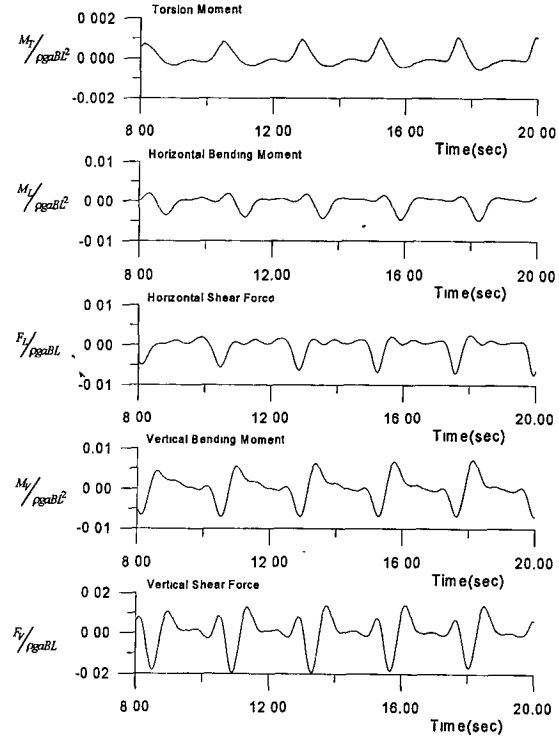

Fig. 12. Time histories of nondimensional wave load (μ=30°, λ/L=1.0, H/λ=1/20, Δt=T/60, N=30, Fr=0.15).

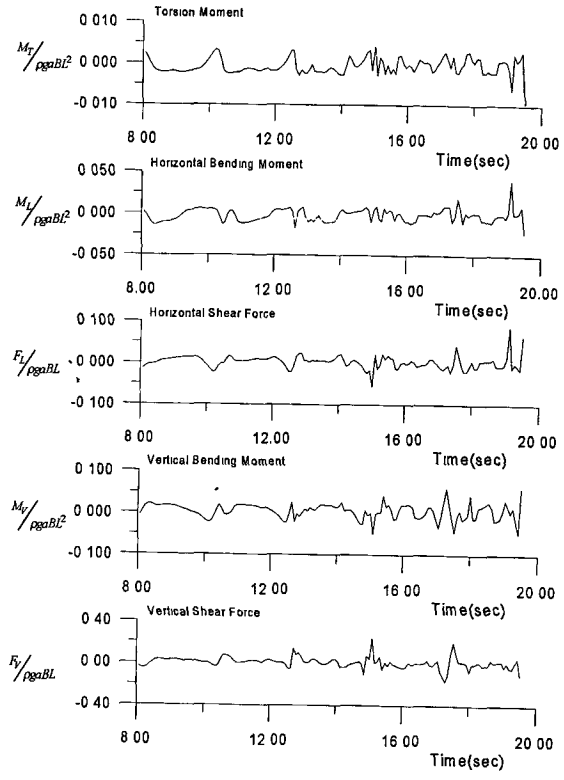

Fig. 13. Time histories of nondimensional wave loads (μ=30°, λ/L=1.0, H/λ=1/20, Δt=T/30, N=60, Fr=0.15).

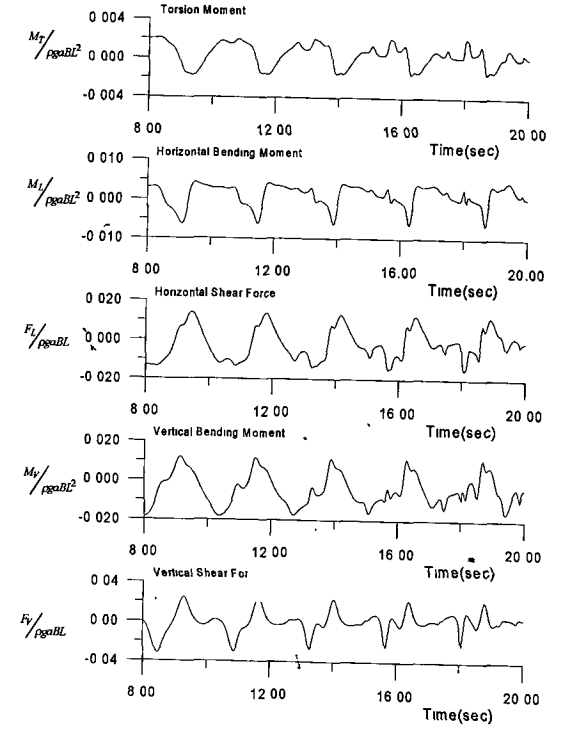

Fig. 14. Time histories of nondimensional wave loads (μ=30°, λ/L=1.0, H/λ=1/20, Δt=T/60, N=90, Fr=0.15).

below the zero level, which means that the ship oscillates in an inclined status to the port side. Similarly, the results for μ=60° with H/λ=1/30 are shown in Figs. 7 and 8 and are also stable without the drifting phenomena. This proves that DFT is really workable for the above two cases. There are some differences between the two cases, but they are not large. The results for the oblique bow wave cases, μ=120°, are shown in Figs. 9 and 10. Again, the results are also quite stable because of the application of DFT. In Fig. 9, the roll motion oscillates above the zero level, which means the ship oscillates in an inclined status to the starboard side. This situation occurs because the wave comes from the port side while it comes from the starboard side for μ=60° as shown in Fig. 7. These results in Figs. 7 and 9 confirmed with the physical phenomena. Comparing the sea load results for these different wave directions, we find that the sea loads for a bow wave are generally larger than those for a stern wave. Furthermore, a special phenomena appears in Fig. 10, which shows two significant peaks in one wave period for all the wave loads except for the torsion moment. This interesting phenomena may be due to the phase difference and the coupling effects of the motions.

In the above calculations using DFT, we had to first decide on the time interval (Δt) and on the number of filters (N). A series of tests was conducted by Fang *et al.* (1996). Figures 11-14 show some examples of the results of the numerical tests with different numbers of filters and time intervals. In the figures, the results appear to become unstable when the number of filters increases. Therefore, from the systematic analysis (Fang *et al.*, 1996), we suggest that the time interval should be 1/60 of the wave period (T), and that the suitable filter number is 30, which was applied in Figs. 3-10.

VI. Summary

A calculating method for the nonlinear sea loads for a ship advancing in waves has been developed in the paper. The method produces results which, in general, can be used by naval architects in ship design. From the above analysis, some conclusions can be drawn as follows:

(1) The ARFT method can be used to retrieve the numerical drifting error in a ship motion but will cause an artificial external force on the ship, making sea load prediction impractical. Hence, the ARFT method may be suitable for prediction of motions but not for prediction of sea loads.

(2) The DFT method not only can avoid the numerical drifting phenomena in ship motion, but

also makes sea load prediction more practical. However, the time interval (Δt) and the number of filters (N) must be selected carefully to make the results stable. The suggested values are 1/60 of the wave period (T) and N=30. However, these suggestions are only suitable for infinite water depth as in the present study. If the water depth is finite, the results may be different.

(3) The results calculated in the time domain show that the nonlinear effect is significant when the wave amplitude increases and can not be neglected.

(4) A technique for predicting sea loads under large wave amplitude has been developed in the paper; however, we still need corresponding experimental data to further confirm its validity.

Acknowledgment

The authors want to express their thanks to the National Science Council, R.O.C. for financial support under contract NSC 85-2611-E006-019. The authors also thank Mr. Lin, Han-Pi for his help in preparing the data.

References

Bø̈rresen, R. and F. Tellsgard (1980) Time history simulation of vertical motions and loads on ships in regular head waves of large amplitude. *Norwegian Maritime Research*, Norway, (2), 2-11.

Chen, S. Y. (1994) *Analysis for the Nonlinear Motion and Dynamic Stability for a Ship Advancing in Oblique Waves*. M.S. Thesis. National Cheng Kung Univ., Tainan, Taiwan, R.O.C.

Fujino, M. and B. S. Yoon (1986) A practical method of estimating ship motions and wave loads in large amplitude waves. *International Shipbuilding Progress*, **33**(385), 159-172.

Fang, M. C., M. L. Lee, and C. K. Lee (1993) Time simulation of water shipping for a ship advancing in large longitudinal waves. *Journal of Ship Research*, **37**(2), 126-137.

Fang, M. C. and S. S. Her (1995) The nonlinear SWATH ship motion in large longitudinal waves. *International Shipbuilding Progress*, **42**(431), 197-220.

Fang, M. C. and C. M. Liao (1996) Predictions of the sea loads for a ship advancing in waves. *Journal of SNAME, R.O.C.*, **15**(2), 35-44.

Fang, M. C., S. X. Su, and Y. Liou (1996) *Time Simulation of Nonlinear Wave Load on a Ship in Oblique Waves*. Report NSC 85-2611-E006-019, National Science Council, R.O C., Taipei, R.O.C.

Gerritsma, J. and W. Beukelman (1967) *Analysis of the Modified Strip Theory for the Calculation of Ship Motions and Wave Bending Moments*. Report 96S, National Ship Research Center, Delft, Netherlands.

Jacobs, W. R. (1958) The analytical calculation of ship bending moments in regular waves. *Journal of Ship Research*, **2**(1), 20-29.

Korvin-Kroukovsky, B. V. (1955) Investigation of ship motions in regular waves. *Tran., SNAME*, **63**, 386-435.

Kim, C. H., F. S. Chou, and D. Tein (1980) Motions and hydrodynamic loads of a ship advancing in oblique waves. *Tran., SNAME*, **88**, 225-256.

Ohtsubo, H., T. Kuroiwa, and Y Tamamoto (1985) Structural response of ships among rough seas-effects of higher frequency vibration and hydrodynamic coefficients (1st Report). *Journal of Society of Naval Architects of Japan*, **157**, 391-400.

Salvesen, N., E. O. Tuck, and O. Faltinsen (1970) Ship motions and sea loads. *Trans., SNAME*, **78**, 250-287.

Tasai, F. and M. Takaki (1969) Theory and calculation of ship responses in regular waves (in Japanese). Symposium on Seaworthiness of Ships, Japan Society of Naval Architects, Tokyo, Japan.

Wahab, R. (1967) *Amidship Forces and Moments on a CB=0.80 Series 60 Model in Waves from Various Directions*. Report 100S, Netherlands Ship Research Center TNO, Delft, Netherlands.

Wahab, R. and J. H. Vink (1975) Wave induced motions and loads of ships in oblique waves. *International Shipbuilding Progress*, **122**(249), 151-184.

Nonlinear Wave Loads in Oblique Waves

斜向波中非線性波浪負荷之時程模擬

方銘川　廖正民

國立成功大學造船及船舶機械工程研究所

摘　要

本論文中提出了一以截片理論爲基礎的方法來預測船隻在斜向波中所受之非線性負荷。由於過去在流體動力學良好的發展，使得流體動力係數及力量可以預估得相當好，因此在本研究中，作著將船體視爲一自由樑，而利用簡樑理論來預估船體之波浪負荷，如彎矩、剪力及扭矩。本文中利用過去發展良好的線性基礎再發展一套分析大波浪中的非線性負荷模式，此外，爲了去掉橫移與橫擺之數值漂移現象，分別利用假想恢復力與數位濾波法之技巧來去除此現象。而一系列之分析中得到一些有用的建議，可供作此類分析者參考。因此本文所發展之計算過程，可視爲預測船體運動與波浪負荷的有效分析工具之一.